

## Numerical Simulation Of Solid Flow Character With The Different Inlet Position Of Ejecting Coal Powder In Cfb With Sct

Jing-yu Ran, Jian-jun Zhou, Ge Pu and Li Zhang

Institute of Energy and Environment, Chongqing University, Chongqing 400044, China

### Abstract

It can reach a highly efficient combustion and a lower pollution for lower rank coal using the Synthetical Combustion Technology (SCT) with CFB. In this paper, considering the mutual interactions between gas and particles, and the particle collisions, the Euler two-fluid model is applied to simulate the gas-particle turbulent flow in a Circulating Fluidized Bed (CFB) reactor with SCT that is adopted the combustion technology of mixed lower rank fuel. The solid flow character has studied with the different inlet position of ejecting coal powder in CFB with SCT and the different inlet velocity of the secondary air. With the different inlet velocity of the secondary air and the position of ejecting coal powder apart from horizontal wind distributed board 2600mm and 2000mm, the velocity of the particle changes much higher and the flow stability is unstable. For the sparse region segment of CFB with SCT, higher particle-concentration can't be formed. Ejecting coal powder position apart from horizontal wind distributed board 2300mm, the flow stability is stable and it can form much higher concentration particle flow in the sparse region segment. And the results have also been shown: to keep the inlet secondary velocity at 2m/s and the disposed inlet position at 2300mm, the CFB with SCT, which is adopted the combustion technology of mixed lower rank fuel, will be formed higher concentration particle flow above the dense phase region, and could make the particles be combusted at higher combustion efficiency. The core-annulus flow structure is still formed in the different position of ejecting coal powder of CFB with SCT.

**Key words:** CFB combined combustion, the solid flow character, numerical simulation, SCT

### Introduction

It is known to all that CFB combustion is regarded as the clean and higher-efficiency technology. Its particular hydrodynamic characteristics and structure has a lot of advantages, such as stronger adaptability to many fuel, higher combustion efficiency, lower pollution and so on<sup>[1-2]</sup>. However, if the coal quality and coal size varied greatly, the combustion stability to the rated load might be become worse<sup>[3]</sup>. In order to solve the several disadvantages that the common CFB burns the lower rank coal, an ejecting pulverized coal combustor and system are added into the CFB combustion system, the ejecting pulverized coal combustor is located between dense phase region and spare phase region of CFB, and this is named Synthetical Combustion Technology(SCT) of CFB, which can strengthen the combustion of the lower rank coal, as well as can enhance the higher temperature of the sparse phase region in the furnace, and can make the lower rank coal combust well. Some scholars have investigated about its combustion characteristic, but little to the gas-solid flow character with different inlet position of ejecting coal powder in the CFB with SCT. Hao et.al<sup>[4-6]</sup> discussed about the feasibility of SCT in the industrial boiler. The SCT is applied in the industrial

boiler, its combustion efficiency can be approximate to the pulverized coal boiler and it also reduces the pollution. Some people<sup>[7-10]</sup> have analyzed the mass and heat transfer, gas-solid flow character in the fluidized bed, and obtained the relation expression to calculate the heat loss of incomplete combustion and solid incomplete combustion. But there is little reference for the CFB with SCT, especial the combustion, flow and heat transfer character for the lower rank fuel (such coal) about this technology is more less attention to. To study gas/solid flow character will be contribution to the understanding of the behavior of the SCT, and can significantly enhance optimum the design, operation and maintenance of the SCT, especially the position of ejecting coal powder of the SCT.

In this paper, considered the mutual interactions between gas and particles, and the particle collisions, the Euler-Euler approach is used to model hydrodynamics of gas and particles phases in the CFB with SCT, the particle flow characteristics with different inlet secondary air velocity and position of ejecting coal powder in the CFB have been investigated.

### Physics and Mathematic Models

#### Physics Model

The investigated physical model is a 35t/h CFB which locates in Chongqing, China, it is shown in Fig.1. The height of the dense phase segment is located in 3 meters from the distribution wind board, the transition segment region is located in between the height of 3 meters and 4 meters from the distribution wind board, that of the spare phase segment is located in higher than 4 meters from the distribution wind board. The margin length of the dense phase segment cross section is 3.2 meters×3.2 meters, and that of the spare phase segment cross section is 3.81 meters×3.81 meters. The position of ejecting coal powder in the CFB with SCT is decided according to the simulation items.

#### Mathematic model

For presenting the governing equations, some items are considered as following: the temperature in gas-solid flow field is stable and equivalent. The mix coordinates system is adopted, that is, the Cartesian coordinates system is applied for the furnace, flue gas passage, and L valve, the cylindrical coordinates system is adopted for the cyclone of the CFB with SCT. The density and viscosity are constant.

Particle Continuity equation:

$$\frac{\partial \rho_k}{\partial t} + \frac{\partial(\rho_k V_{kj})}{\partial x_j} = s_k = n_k \frac{d}{dt} \left( \frac{\pi d_k^3}{6} \frac{n_k m_k}{\phi_k} \right) \quad (1)$$

Particle N-S equation:

$$\frac{\partial(\rho_k V_{ki})}{\partial t} + \frac{\partial(\rho_k V_{ki} V_{kj})}{\partial x_j} = \rho_k g_i + 18\mu \rho_k (U_i - V_{ki}) \left( 1 + \frac{Re_k^{2/3}}{6} \right) / d_k^2 \frac{n_k m_k}{\phi_k} + U_i s_k + F_{k,Mi} \quad (2)$$

Gas Continuity equation:

$$\frac{\partial \rho}{\partial t} + \frac{\partial(\rho U_j)}{\partial x_j} = s = - \sum n_k \frac{d}{dt} \left( \frac{\pi d_k^3}{6} \frac{n_k m_k}{\phi_k} \right) \quad (3)$$

Gas N-S equation:

$$\frac{\partial(\rho U_i)}{\partial t} + \frac{\partial(\rho U_i U_j)}{\partial x_j} = -\frac{\partial p}{\partial x_i} + \frac{\partial}{\partial x_j} \left[ \mu \left( \frac{\partial U_j}{\partial x_i} + \frac{\partial U_i}{\partial x_j} \right) \right] + \Delta \rho g_i + \sum_k 18\mu\rho_k (V_{ki} - U_i) \left( 1 + \frac{Re_k^{2/3}}{6} \right) / d_k^2 \frac{n_k m_k}{\phi_k} + U_i S + F_{Mi} \quad (4)$$

Where,  $\rho$  is the gas density,  $p$  is the static pressure,  $\mu$  is the effective viscosity,  $\mu = \mu_l + \mu_T$ .  $\mu_l$  is the laminar viscosity,  $\mu_T$  is the turbulent viscosity. For the strong turbulent flow,  $\mu_T \gg \mu_l$ , that is  $\mu = \mu_T = C_{\mu} \rho k^2 / \varepsilon$ ;  $k$  and  $\varepsilon$  are turbulent kinetic energy and its dissipated turbulent kinetic energy of the flow respectively. The relative Renault number and the Magnus force can be shown as follow:

$$Re_k = (V_{ki} - U_i) d_k / \left( \frac{1}{3} v_k + \frac{2}{3} \frac{\mu}{\rho} \right) \quad (5)$$

$$F_{Mi} = -\sum F_{k,Mi} = \sum -\frac{\pi}{16} d_k^3 \frac{\mu}{\rho} (\nabla \times U_j) \quad (6)$$

$$(U_i - V_{ki}) = \sum \frac{\pi}{16} d_k^3 \frac{\mu}{\rho} (U_i - V_{ki}) \left( \frac{dU_i}{dx_i} - \frac{dV_{ki}}{dx_i} \right)$$

There still needs other equations to close the above equations. The RNG based  $k-\varepsilon$  turbulence model is derived from the instantaneous Navier-Stokes equations, using a mathematical technique called "renormalization group" (RNG) methods. The analytical derivation results in a model with constants different from those in the standard  $k-\varepsilon$  model, and additional items and functions in the transport equations for  $k$  and  $\varepsilon$ . The RNG  $k-\varepsilon$  model has a similar form to the standard  $k-\varepsilon$  model:

$$\frac{\partial}{\partial t} (\rho k) + \frac{\partial}{\partial x_i} (\rho k u_i) = \frac{\partial}{\partial x_i} \left( \frac{\mu_e}{\sigma_k} \frac{\partial k}{\partial x_i} \right) + G_k - \rho \varepsilon \quad (7)$$

$$\frac{\partial}{\partial t} (\rho \varepsilon) + \frac{\partial}{\partial x_i} (\rho \varepsilon u_i) = \frac{\partial}{\partial x_i} \left( \frac{\mu_e}{\sigma_{\varepsilon k}} \frac{\partial \varepsilon}{\partial x_i} \right) + \quad (8)$$

$$\frac{\varepsilon}{k} (C_{\varepsilon 1} C_k - C_{\varepsilon 2} \rho \varepsilon)$$

The model constant:

$$C_u = 0.085, C_{\varepsilon 2} = 1.68.$$

$$\sigma_k = 0.7179, \sigma_{\varepsilon} = 0.7179.$$

### Grid and numerical method

The bottom of the furnace, and the cyclone separator as well as riser and stuff back-feeder were used non-uniform mesh, but the transmit phase zone is regular and uses the uniform mesh to improve the mesh quality. The cross grids are set up (see Fig.1, the technology about adding grid density in local part and coupling grid in different segment are adopted. The

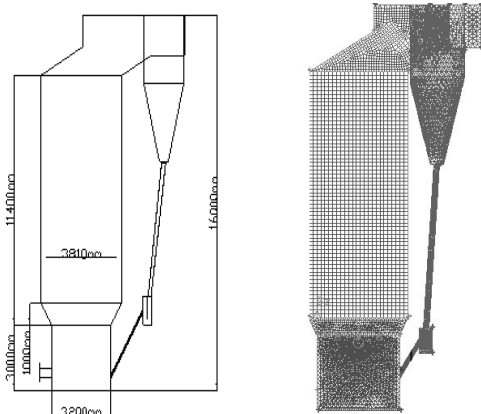


Fig1. Geometric model and mesh

object was meshed about 450,000 fluid cells.

Conservation equations of mass and momentum are described using the Eulerian- Eulerian approach<sup>[11,12]</sup>, and are solved simultaneously. This approach treats each phase separately, and the only link between the two phases is through the drag force in the momentum equations. The discretization scheme for the convection terms in the momentum equations uses the power law interpolation scheme which provides a formal accuracy between first and second order. This scheme is more robust and less computationally intensive than higher-order schemes. The gas governing equations are solved using the well-known SIMPLE algorithm<sup>[13]</sup>. A CFB with SCT system is used in which the convection and diffusion terms are discretized using the front separated method and central-difference method respectively. The source items are also linearized. The finite difference equations are solved using the Gauss-Seidel method under-relaxation iteration. The particle equations are solved using the Gill method.

### Initial and boundary conditions

According to character of the CFB with SCT, the simulation items are decided and listed in Table 1,  $V_{pa}$  is the primal air velocity,  $V_{sa}$  is the second air velocity. The bed material that is used in the simulation is sands, whose average diameter is 0.6mm, and the density is 2500kg/m<sup>3</sup>. The air density is 1.2kg/m<sup>3</sup>. Initial, at the inlet, all velocities and volume fractions of both gas and solid phase are specified. The pressure is not specified at the inlet because of the incompressible gas phase assumption (relatively low pressure drop system). At the outlet, only the pressure is specified (atmospheric). The other variables are subject to the Newmann boundary condition. For the wall, the gas tangential and normal velocities are set with zero (non-slip condition). The tangential and normal velocity of the solid are also set with zero. The following boundary equations apply for the solid tangential velocity and granular temperature near the wall<sup>[14]</sup>:

$$v_{s,w} = -\frac{6\mu_s \varepsilon_{s,max}}{\sqrt{3\pi\phi\rho_s \varepsilon_s g_0} \sqrt{\Theta_s}} \frac{\partial v_{s,w}}{\partial n}$$

$$\Theta_{s,w} = -\frac{k_s \Theta_s}{\gamma_{s,w}} \frac{\partial \Theta_{s,w}}{\partial n} + \frac{\sqrt{3\pi\phi\rho_s \varepsilon_s} v_{s,slip}^2 g_0 \Theta_s^{3/2}}{6\varepsilon_{s,max} \gamma_{s,w}}$$

The equations are developed by Hui et al. <sup>[14]</sup>, and Johnson and Jackson <sup>[15]</sup>. According to their work, the slip velocity between

items	Ejecting coal powder position(h) and bed material height(H)		$V_{pa}/ms^{-1}$	$V_{sa}/ms^{-1}$
	h/mm	H/mm		
1	2600	400	2	20
2	2600	400	2	25
3	2600	400	2	30
4	2300	400	2	20
5	2300	400	2	25
6	2300	400	2	30
7	2000	400	2	20
8	2000	400	2	25
9	2000	400	2	30

Table1 Simulation items

particles and the wall can be obtained by equating the tangential force exerted on the boundary and the particle shear stress close to the wall. Similarly, the granular temperature at the wall is obtained by equating the granular temperature flux at the wall to the inelastic dissipation of energy, and to the

generation of granular energy due to slip at the wall region. These boundary conditions are successfully applied to dense riser flow.

### Results and Discussions

The average velocity of the particle ( $V_{ap}$ ) for the Z-axis at the different ejecting coal powder position and the different second air velocity are shown in Fig.2-4. The velocity is increased firstly, then it falls down, and at last it rises up near the exit with increasing the bed height ( $H_b$ ) of CFB with SCT. The maximum  $V_{ap}$  is appeared near the position where  $H_b=4000\text{mm}$ , because the secondary air is entered, which makes the  $V_{ap}$  increases highly. After a certain distance, the

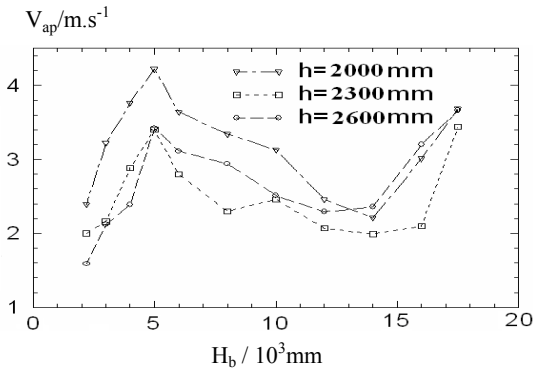


Fig.2 Average velocity of the particle at different ejecting coal powder position at the velocity of the second air is 25m/s

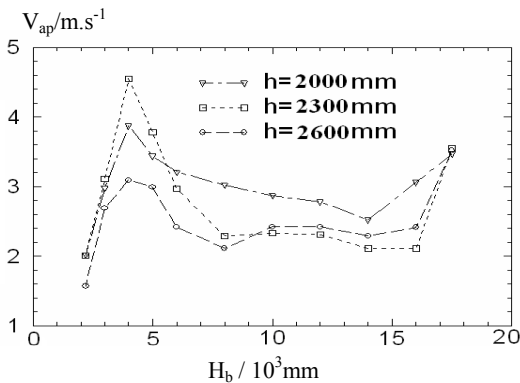


Fig.3 Average velocity of the particle at different ejecting coal powder position at the velocity of the second air is 30m/s

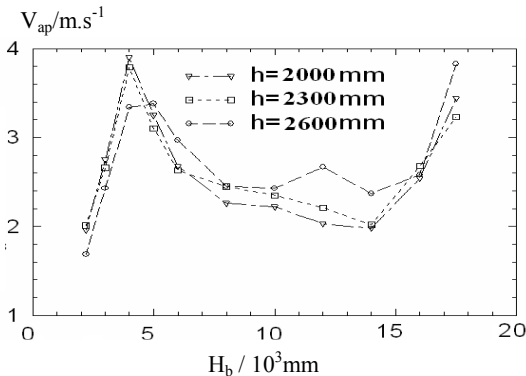


Fig.4 Average velocity of the particle at different ejecting coal powder position at the velocity of the second air is 35m/s

$V_{ap}$  is changed little, the reason is that the material particles is accelerated from the horizontal primo-air distribution board,

the drag force become smaller with increasing the  $V_{ap}$ . In the

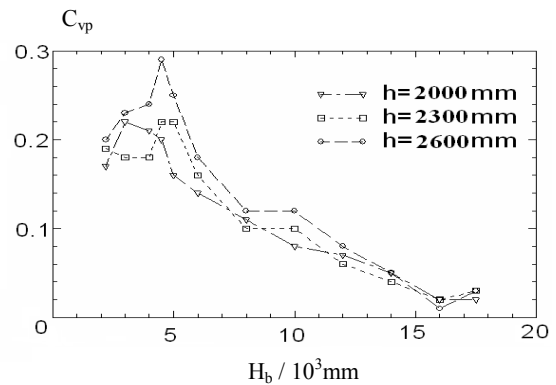


Fig.5 Distribution of the volume concentration of the particle at the velocity of the second air is 25m/s

spare phase segment, the influence of gravity is bigger than that of the drag force, the change rate of the  $V_{ap}$  decrease gradually. Meanwhile, the factors of suddenly changing flow direction and the decreasing outlet area size make the  $V_{ap}$  become bigger. For the three different ejecting coal powder position ( $h$ ), the  $V_{ap}$  of spare phase segment have changed more little at the different  $V_{sa}$  while the ejecting coal powder position ( $h$ ) is 2300mm.

In addition, form the Fig.2-4, the maximum  $V_{ap}$  is relative to

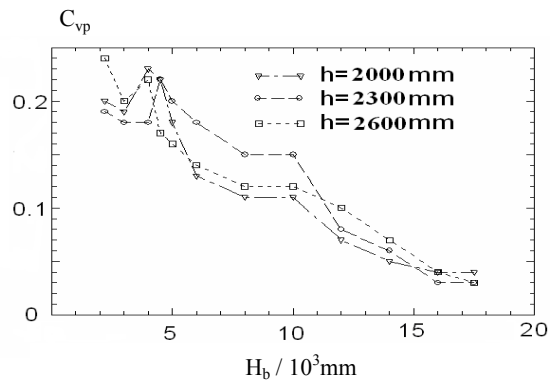


Fig.6 Distribution of the volume concentration of the particle at the velocity of the second air is 30m/s

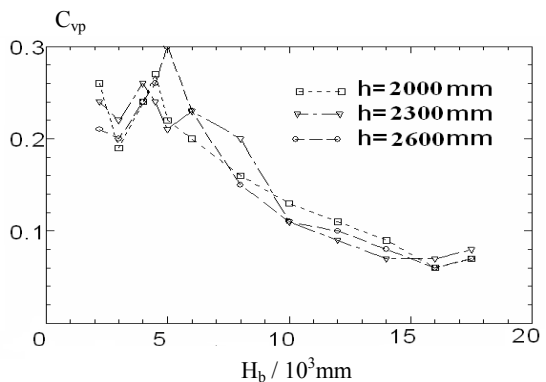


Fig.7 Distribution of the volume concentration of the particle at the velocity of the second air is 35m/s

the secondary air velocity, the bigger of the secondary air velocity is, the bigger of the maximum  $V_{ap}$  is. However, for the spare phase segment, the higher secondary air velocity and the lower particle flow velocity are appeared, espially, the particles' backflow are happened near the wall, the  $V_{ap}$

decreases, which is useful for adding the particles' stay time in CFB with SCT.

Fig.5-7 shows that the influence of the volume concentration of the particle ( $C_{vp}$ ) at the different secondary air velocity and different ejecting coal powder position ( $h$ ). The  $C_{vp}$  increases with increasing the bed height ( $H_b$ ) of the CFB firstly, but it decreases while the  $H_b$  is bigger than the height of the secondary air inlet position. It increases near the outlet of the CFB, because outlet section areas size becomes smaller.

From the Figures 5-7, the position where the maximum of the  $C_{vp}$  is occurred is changed with the different inlet position of ejecting coal powder ( $h$ ), because an added coal powder feeder

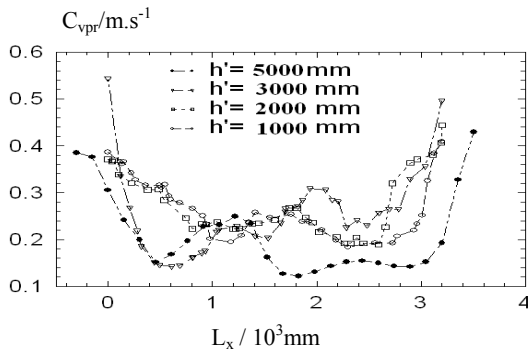


Fig.8 Distribution of the volume concentration of the particle in different height of CFB at ejecting coal powder position -300mm the velocity of the second air is 35m/s

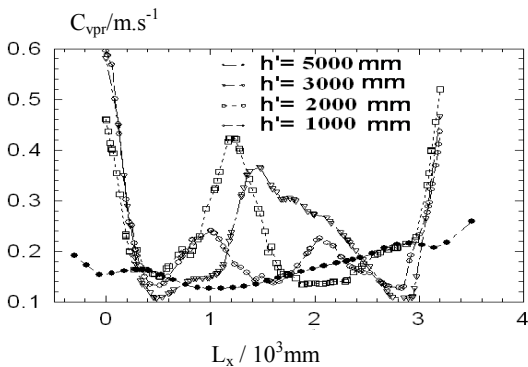


Fig.9 Distribution of the volume concentration of the particle in different height of CFB at ejecting coal powder position -600mm the velocity of the second air is 35m/s

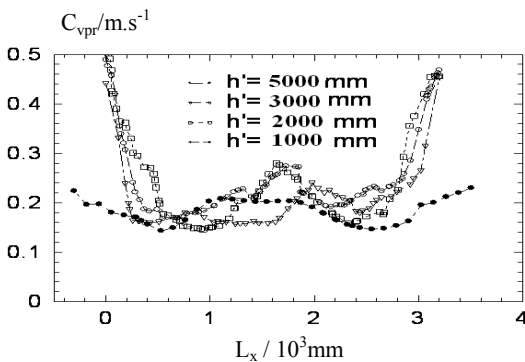


Fig.10 Distribution of the volume concentration of the particle in different height of CFB at ejecting coal powder position -900mm the velocity of the second air is 35m/s

which makes the particle concentration increases temporarily. While the ejecting coal powder position  $h$  is 2600mm, the maximum of the  $C_{vp}$  is appeared at  $H_b$  with 3000mm. And for the ejecting coal powder position  $h$  with 2000mm is so close

to the back-feeder position that will decrease the  $C_{vp}$  of the transition region segment, which could result in ignition problem. When the ejecting coal powder position is 2300mm, the  $C_{vp}$  in the transition region segment is higher than that of the others.

With different ejecting coal powder position  $h$  but the same secondary air velocity (35m/s), the  $C_{vp}$  with the different height ( $h'$ ) section of CFB ( $h'=1000$ mm, 2000mm, 3000mm and 5000mm from the distribution wind board) is shown in Fig.8-10. For the different  $h'$ , the volume concentration of the particle in radial ( $C_{vpr}$ ) in the core-region of the section is smaller than that of the near wall region. Meanwhile, the  $C_{vpr}$  changes a little with  $h'=2000$ mm and 3000mm, because  $h'=2000$ mm is located near the ejecting coal powder feeder inlet position and  $h'=3000$ mm is located near the secondary air inlet, and the distribution of the  $C_{vpr}$  likes wave-style for these two  $h'$ . For the other  $h'$ , the wave character is not obviously. The change range of the  $C_{vpr}$  with the ejecting coal powder position  $h=2300$ mm is bigger than that of the other two. And for the  $h=2000$ mm, the entering coal position is close to the back-feeder position, it can't combust layered. However, the core-annulus structure flow character is occurred in the simulation results.

## Conclusions

Considering the mutual interactions between gas and particles, and the particle collisions, the Euler two-fluid model is applied to simulate the gas-particle turbulent flow in a CFB with SCT. The characters for flow and volume concentration distribution of particles are studied in different secondary air velocity and ejecting coal powder position, some results are reached.

The average velocity of the particle ( $V_{ap}$ ) for the Z-axis is different with the ejecting coal powder position and the different second air velocity, the change of the  $V_{ap}$  in spare phase segment is smaller at the different  $V_{sa}$  while the ejecting coal powder position ( $h$ ) is 2300mm.

The volume concentration of the particle ( $C_{vp}$ ) is influenced by the different positions of ejecting coal powder. While the position of ejecting coal is placed between the inlet of the secondary air and the inlet of back-feeder of CFB with SCT, it can form higher concentration particle flow. If the position of ejecting coal powder is located in 2300mm depart from the distribution wind board, the higher concentration particle flow could be formed, which could increase the combustion temperature and make the fuel combust in the high temperature. The higher concentration particle flow for the other position ( $h=2000$ mm or  $h=3000$ mm) of ejecting coal powder isn't obviously.

The core-annulus flow structure is still formed in the different position of ejecting coal powder. The higher concentration particle flow in the transmit segment region can form in the CFB with SCT. When the position of ejecting coal powder is 2300mm and the secondary air velocity is 35m/s, the flow stability is stable and much higher concentration particle flow in the sparse region segment is occurred to.

## Acknowledgments

This work is supported by the government of Chongqing city, China under Project No. 05-1GX-QT194.

## References

- [1] Zhu kaiqiang, Rui xinhong, Equipments and systems of circulating fluidized bed boiler, CEPP, Beijing, 2004
- [2] Grace J.R., Avidan A.A. and Knowlton T.M.. Circulating Fluidized beds. Published by Blackie Academic & Professional, New York, USA, 1997.

- [3] Daizo Kunii, and Octave Levenspiel. Fluidization Engineering. 2nd. Published by Butterworth-Heinemann, Newton, MA, USA, 1991
- [4] Hao Zhijin, Jiang Xiuming, Wang Qing et al. Application of In-Furnace Combined Circulation Combustion Technology in Retrofit of Industrial Boilers. J. Boiler Technology, 1999, 30[9]:30-32.
- [5] JIANG Shaojun, SUN Qingbin. Retrofit of Travelling Grate Boiler Based on Combined Combustion Technology. J. Boiler Manufacturing, 2004, 8:58-59
- [6] Wang Qun, Pan Minglin. Renovation of Cha in-Grate Boiler With Pulverized Coal Combined Combustion[J]. Power System Engineering, 1997, 13(2):53-57
- [7] Zhao Guangbo, Zhu Qunyi, Yun Xiaoyin, et al. The Material and Heat Balance of a Dual-fuel Pulverized Coal-fired Fluidized Bed Multiple Combustion Boiler[J]. Journal of Engineering for Thermal Energy & Power, 1997, 12(1), 8-10
- [8] ZHAO Guangbo, QIN Yukun. Method for Heat Transfer Calculation in Furnace of Fluidized Bed-Pulverized Coal Combined Combustion Boiler. J. Power Engineering, 2000, 20(4), 740-744, 759
- [9] Zhao Guangbo, Huang Yimin, GAO Zhihong et al. Effect of Load Distribution on Thermal Dynamics of CFB Combining with Pulverized Coal Firing[J]. Power System Engineering, 1998, 14(3):7-11, 15
- [10] Benyahia S., Arastoopour H., Knowlton T.M., Two-dimensional transient numerical simulation of solids and gas flow in the riser section of a circulating fluidized bed, Chem. Eng. Commun. 189 (2002) 510-527.
- [11] BENAHAIA S, ARASTOOPOUR H, M KNOWLTON T, et al. Simulation of particles and gas flow behavior in the riser section of a circulating fluidized bed using the kinetic theory approach for the particle phase. J. Powder Technology, 2000, 112 : 24-33.
- [12] ARASTOOPOUR H. Numerical simulation and experimental analysis of gas/ solid flow systems : 1999 Fluor-Daniel Plenary lecture. J. Powder Technology, 2001, 119:59-67.
- [13] MOUKALLED F, DARWISH M, SEKAR B. A Pressure-based algorithm for multi2phase flow at all speeds. Journal of Computational Physics, 2003, 190 (2):550-571.
- [14] Hui K., Haff P.K., Jackson R., Boundary conditions for high-shear grain flows, J. Fluid Mech. 145(1984) 223-233.
- [15] Johnson P.C., Jackson R., Frictional-collisional constitutive relations for granular materials, with application to plane shearing, J. Fluid Mech. 176\_1987.67-93.